GEOMATICS AND ENVIRONMENTAL ENGINEERING • Volume 15 • Number 1 • 2021

https://doi.org/10.7494/geom.2021.15.1.41

Adetola Olufunmilayo Gbopa[1], Emmanuel Gbenga Ayodele[2],
Chukwuma John Okolie[3], Akinwumi Olaitan Ajayi[4], Chima Jude Iheaturu[5]

Unmanned Aerial Vehicles for Three-dimensional Mapping and Change Detection Analysis[6]

Abstract: Unmanned Aerial Vehicles (UAVs), commonly known as drones are increasingly being used for three-dimensional (3D) mapping of the environment. This study utilised UAV technology to produce a revised 3D map of the University of Lagos as well as land cover change detection analysis. A DJI Phantom 4 UAV was used to collect digital images at a flying height of 90 m, and 75% fore and 65% side overlaps. Ground control points (GCPs) for orthophoto rectification were coordinated with a Trimble R8 Global Navigation Satellite System. Pix4D Mapper was used to produce a digital terrain model and an orthophoto at a ground sampling distance of 4.36 cm. The change detection analysis, using the 2015 base map as reference, revealed a significant change in the land cover such as an increase of 16,306.7 m^2 in buildings between 2015 and 2019. The root mean square error analysis performed using 7 GCPs showed a horizontal and vertical accuracy of 0.183 m and 0.157 m respectively. This suggests a high level of accuracy, which is adequate for 3D mapping and change detection analysis at a sustainable cost.

Keywords: UAV technology, 3D mapping, orthophoto, land cover, change detection analysis

Received: 27 September 2020; accepted: 10 November 2020

[1] University of Lagos, Department of Surveying and Geoinformatics, Nigeria, email: geogbopa@gmail.com, ORCID ID: https://orcid.org/0000-0003-2476-573X
[2] University of Lagos, Department of Surveying and Geoinformatics, Nigeria, email: eayodele@unilag.edu.ng, ORCID ID: https://orcid.org/0000-0003-2684-2276
[3] University of Lagos, Department of Surveying and Geoinformatics, Nigeria, email: cjohnokolie@gmail.com, ORCID ID: https://orcid.org/0000-0003-4542-7051
[4] University of Lagos, Department of Surveying and Geoinformatics, Nigeria, email: papaj4christ@gmail.com, ORCID ID: https://orcid.org/0000-0001-9135-1153
[5] Imo State University, Department of Surveying and Geoinformatics, Nigeria, email: chima.geomaven@gmail.com, ORCID ID: https://orcid.org/0000-0003-0472-9715
[6] This research did not receive any specific funding from the public, private or not-for-profit sectors.

1. Introduction

Three-dimensional (3D) mapping is described as the process of gathering locational information and possibly the attributes of features such as roads and buildings, and the representation of such in three dimensions (latitude, longitude and height above sea level) that can be interpreted by a user [1]. According to [2], 3D data acquisition in urban/sub-urban areas requires planning based on classic standards and the application of a variety of surveying methods. Conventional mapping techniques include triangulation, trilateration, traversing, levelling, and radiation [3, 4], while modern techniques include total station surveying, aerial photogrammetry, Global Positioning Systems (GPS) or Global Navigation Satellite Systems (GNSS) surveys, and remote sensing (RS) [5].

In RS, the characteristics of objects or features can be studied using data collected from remote observation points [6]. Also, in photogrammetry, the size, shape and location of objects can be determined using measurement in a single image, a stereo pair or in a block of two or more images. However, measurements done in one image can only give two-dimensional (2D) coordinates, while 3D coordinates can be obtained using two or more images of the same object, captured from different positions. This is called stereoscopic viewing or stereo photogrammetry [7]. The images used in photogrammetry can be captured by various sensors on-board platforms such as manned aircraft (fixed wing or rotary) and satellites. However, operating these technologies involve huge investments beyond the resource base of many individuals. In response, Unmanned Aerial Vehicle (UAV) surveys have emerged as an alternative to the classical manned aerial photogrammetric surveys [1].

Several authors have highlighted the advantages of UAVs that include: rapid data collection for site inspection, surveillance, mapping, 3D modelling and real-time data capture with high geometric resolution under good atmospheric conditions [8–11]. Deliverables of UAV surveys that include orthophotos, 3D point clouds, and digital surface models have wide applications. For example, orthophotos are very useful for manual or semi-automatic feature extraction for map creation or updating [11], as well as for change detection studies [11, 12]. Urban change detection is important for city monitoring and disaster response, as well as the updating of maps and three-dimensional models [13, 14]. The applications of UAV data for change detection analysis present obvious advantages in terms of spatio-temporal resolution and cloudlessness compared to satellite RS images [15]. As noted by [16] and [17], images with high spatial resolution are specially preferred for the accurate processing of variations in urban land cover. This requirement can be met by UAVs through the provision of precise data measurements [18, 19].

The setting of the present study is the University of Lagos in Lagos, Nigeria. This is an ideal location since there are no restrictions imposed on the UAV surveys conducted for the purpose of teaching and research. In addition, the university is growing both in terms of its human population and infrastructure, as evidenced

by changes in land cover and developmental activities. Accordingly, there is a need for up-to-date spatial information of the university to support planning, development and decision making. This study utilised UAV technology to produce a three--dimensional map of the University of Lagos, which will be useful for comprehensive planning and design, development and monitoring as well as to understand the changes in land cover overtime so as to support informed decisions. To achieve this, a UAV-photogrammetric survey was carried out in the University of Lagos main campus, together with ground control survey using Differential GPS (DGPS).

2. Methodology

2.1. Study Area

The study area is the University of Lagos, Akoka in the Lagos Mainland Local Government Area (LGA) of Lagos State, Nigeria. The campus is located between longitudes 3°23'00" E – 3°24'30" E and latitudes 6°30'00" N – 6°31'30" N. It is located in the centre of the metropolis of Lagos, and is low-lying with variations in terrain relief, which makes it susceptible to flooding during rainfall. Figure 1 presents the location map of the University of Lagos, Nigeria.

The University of Lagos is bounded to the east by the Lagos Lagoon and surrounded by densely populated, built-up areas. The university has a growing student population, faculties and other academic and research infrastructure, including recreational facilities and parking spaces, religious buildings, restaurants, and residential buildings. This study area was selected primarily due to its accessibility and the avoidance of the need to obtain a flight permit, which may hinder or delay the execution of the project elsewhere. The size of the total image collection area was approximately 281 hectares.

2.2. Equipment

A low-cost UAV (DJI Phantom 4 Professional) with a maximum flight time of approximately 30 minutes was used for the aerial data acquisition. The camera lens of the UAV has an 84° field of view (FOV), and a focal length of 8.8 mm/24 mm (35 mm format equivalent). The gimbal has a controllable range of −90° to +30° and a maximum controllable angular speed of 90°/s. The UAV system also has an in-built positioning system that can track both Global Positioning System (GPS) and GLONASS satellites. With GPS positioning, the hover accuracy range is ±0.5 m (vertical) and ±1.5 m (horizontal). Prior to the survey, the UAV was checked and evaluated to ensure it was in good condition in accordance with any survey project involving instrumentations. A Trimble R8 GNSS was used to determine the coordinates of the Ground Control Points (GCPs). Table 1 presents the list of all the hardware and software used, such as GNSS receiver and solutions, UAV and Pix4D Mapper used in the study, and their respective functions.

Fig. 1. Map showing the location of University of Lagos (UNILAG).
The western boundary is defined by a canal which is visible on the image.
The water body on the eastern flank is the Lagos Lagoon

Table 1. List of hardware and software used and their functions

Component	Name	Function
Hardware	Trimble R8 GNSS with accessories	For determining the coordinates of GCPs
	DJI Phantom 4 Professional UAV with accessories	Image acquisition
	Tablet (iPad)	Flight planning
	HP Laptop	For processing and information presentation
Software	Google Earth	Pre-mission flight planning
	AutoCAD	Pre-mission flight planning
	Drone Deploy software	Tablet (iPad) integrated software for flight planning
	GNSS Solutions	To download and process the GPS data
	ArcGIS 10.2	GIS software for geospatial analysis and visualisation
	Pix 4D Capture and Pix 4D Mapper	Photogrammetric software used for image processing

2.3. Field Survey

Ground Control Points

The field survey included the measurement of the Ground Control Points (GCPs) using dual frequency GNSS receivers, and acquisition of aerial photographs using DJI Phantom 4 UAV.

Fourteen GCPs, namely XST 347, YTT 28/186, GME 2, PD UN01, etc., which are well spread out were signalised in the study area. Figure 2 shows a view of two signalised GCPs, YTT 28/186 and XST 347. White emulsion paint was used to make cross markings on the GCPs to make them visible from a high altitude. The dimension of the cross markings were approximately 80–100 cm in length and 15–20 cm in width. Static GNSS observation of about 30–40 minutes occupation time was then carried out on each of the GCPs. Figure 3 shows the spatial distribution of the signalised GCPs with Google Earth imagery as the backdrop.

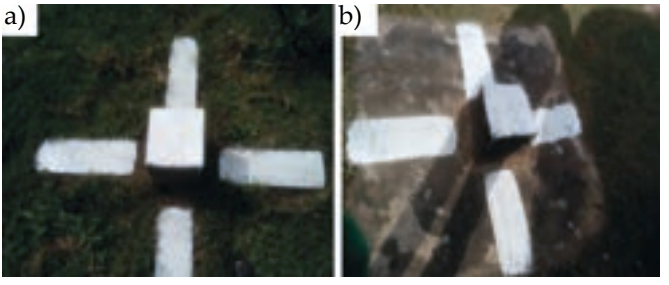

Fig. 2. Some of the GCPs within the University of Lagos used for orthophoto rectification: a) YTT 28/186; b) XST 347

Fig. 3. Spatial distribution of the signalised GCPs shown on Google Earth

UAV Flight

After the pre-marking and measurement of the GCPs, the study area was sub--divided into different missions within AutoCAD software and converted into Key-hole Markup Language (KML) files, which were subsequently loaded into Drone Deploy software for the flight mission. The UAV flight was conducted in a systematic manner based on the partitions to maximize efficiency. The following parameters were set in accordance with standard recommendations: a flying altitude of 90 m, a speed limit of 15 m/s, flight direction of 126°, and overlaps of 75% fore, and 65% side. With the stated specifications, it takes 8 to 15 minutes to cover 15 hectares, which means that the total area can be covered in less than 5 hours of continuous flight. However, continuous flight was not possible due to battery limitations, intervisibility and other logistics. During the survey, the UAV was monitored to ensure it was within the range of visual contact as any other aerial object must be avoided as noted by [7]. Changing weather conditions were also monitored to ensure quality data acquisition, since strong winds adversely affect the operation of UAVs. Summarily, once the UAV had passed its first waypoint (flight path), the next waypoint was initiated. Subsequently, the UAV acquired data following the pre-programmed flight paths. After passing the last waypoint on the flight lines, the UAV terminated its flight plan and initiated

a normal landing sequence, whilst landing at the starting position. Figure 4 presents the 2015 land cover base map of the study area showing some prominent locations. Figure 5 shows a UAV landing/taking-off at two locations within the study area.

Fig. 4. The 2015 land cover base map of University of Lagos

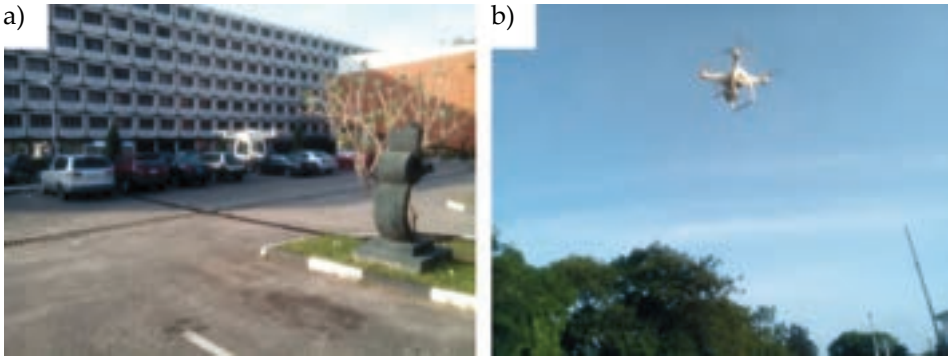

Fig. 5. UAV survey operation: a) landing at the Faculty of Arts; b) take-off

2.4. Data Processing

After the completion of the static GNSS survey, the GNSS receivers were taken to the laboratory for data downloaded and post-processing. The receivers were connected to the computer and the data was downloaded. Trimble Business Centre v3.5 was launched and the project settings including definition of the coordinate system/datum to WGS84 UTM Zone 31N were set. The downloaded data was then imported into the software environment and the coordinates of the base station were inputted. The baseline processing was carried out and the report of the post-processed coordinates was generated and saved as a comma separated variable (CSV) file. Figure 6 shows the final plot of GCPs after the baseline processing.

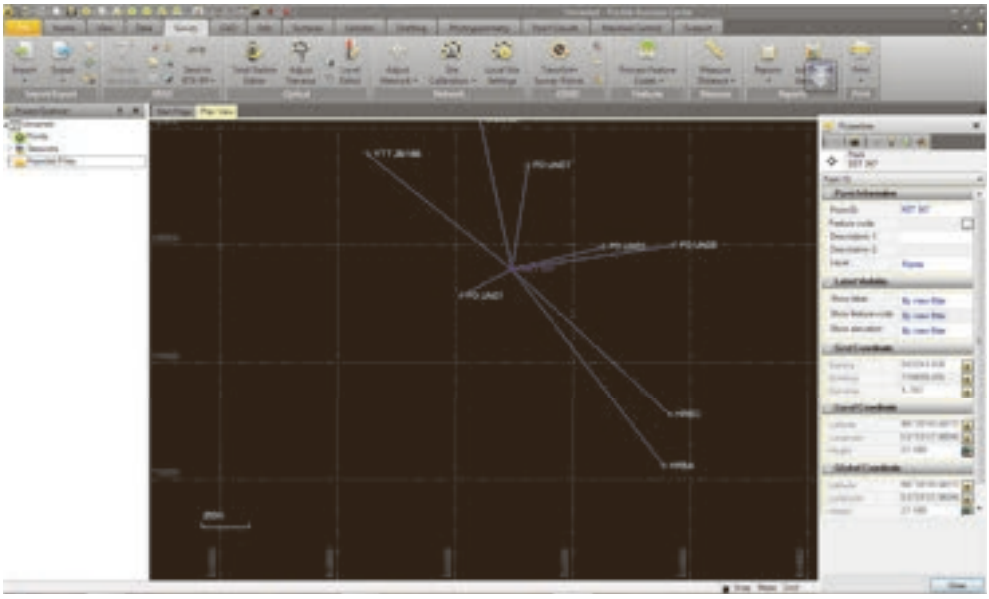

Fig. 6. Final plot of GCPs after baseline processing

The raw photos captured from the UAV flights were downloaded and processed using Pix4D Mapper software. The key stages of the processing workflow adopted in Pix4D Mapper are already well documented in [20]. Essentially, the processing involved initial processing, which handles the image alignment; geo-rectification with GCPs using Pix4D's rayCloud editor, which enables one to justify the precise position of each GCP using the original 2D images, the processing of point cloud and mesh, and the generation of the orthophoto and Digital Terrain Model (DTM). After the processing was completed, the orthophoto that was generated was imported into ArcMap software (Fig. 7) where three main land cover features (buildings, water bodies and vegetation) were vectorised on the orthophoto and displayed in the form of a map.

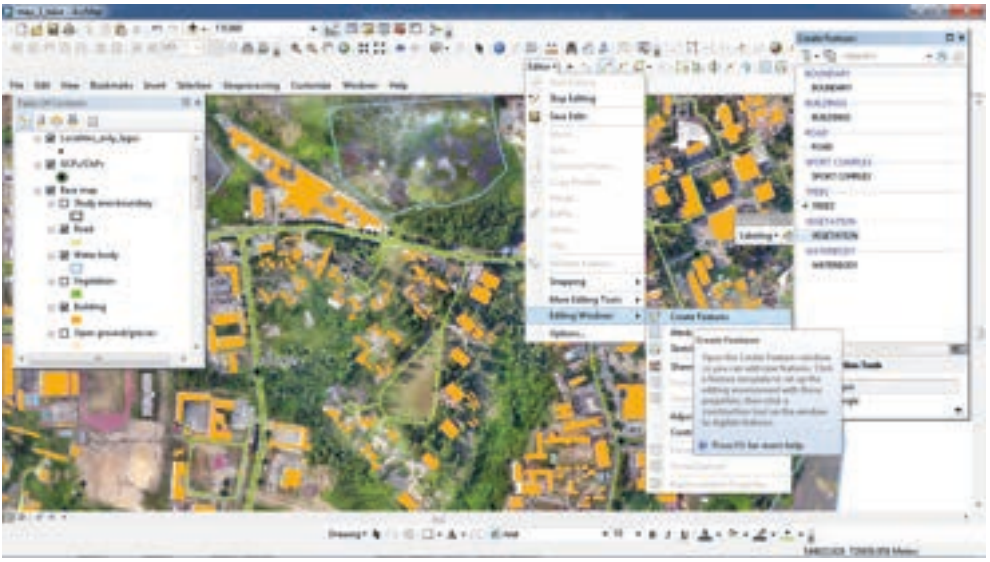

Fig. 7. The land cover features vectorisation in ArcMap software

2.5. Accuracy Assessment

In this study, a point-to-point validation method was used. This technique is based on data points that compare two point clouds directly as identified by [21, 22]. The horizontal and vertical accuracy was validated using the root mean square error (RMSE) and the standard deviation (SD) of the coordinates of the GCPs compared with their positions on the image in line with the literature. The formula for RMSE is as follows:

$$\mathrm{RMSE} = \sqrt{\frac{\sum (N_i - N_j)^2}{n}} \tag{1}$$

where N_i are the observed values, N_j are reference values and n is number of points. The horizontal RMSE (RMSE_r) is given as:

$$\mathrm{RMSE}_r = \sqrt{\frac{\sum \left[(X_i - X_j)^2 + (Y_i - Y_j)^2 \right]}{n}} \tag{2}$$

Equation (2) can also be expressed as Equation (3) below:

$$\mathrm{RMSE}_r = \sqrt{(\mathrm{RMSE}_X)^2 + (\mathrm{RMSE}_Y)^2} \tag{3}$$

In Equation (3):

$$\mathrm{RMSE}_X = \sqrt{\sum \frac{(X_i - X_j)^2}{n}} \tag{4}$$

$$\mathrm{RMSE}_Y = \sqrt{\sum \frac{(Y_i - Y_j)^2}{n}} \tag{5}$$

X_i – the easting coordinate of observed check point,
X_j – the easting coordinate of the orthophoto check point,
Y_i – the northing coordinate of observed check point,
Y_j – the northing coordinate of the orthophoto check point,
n – the number of check points.

According to the National Standard for Spatial Data Accuracy [23], the method for evaluating horizontal accuracy is classified under two conditions. The first condition is that if $\mathrm{RMSE}_X = \mathrm{RMSE}_Y$, then:

$$\textit{Horizontal Accuracy} = 1.7308 \cdot \mathrm{RMSE}_r \tag{6}$$

The second condition is that if $\mathrm{RMSE}_X \neq \mathrm{RMSE}_Y$ and $\mathrm{RMSE}_{min}/\mathrm{RMSE}_{max}$ is between 0.6 and 1.0 (where RMSE_{min} is the smaller value between RMSE_x and RMSE_y and RMSE_{max} is the larger value), circular standard error (at 39.35% confidence) may be approximated as $0.5 \cdot (\mathrm{RMSE}_X + \mathrm{RMSE}_Y)$ [23, 24]. If error is normally distributed and independent in each of the *x*- and *y*-component and error, the accuracy value according to [23] may be approximated according to the following formula:

$$\textit{Horizontal Accuracy} = 2.4477 \cdot 0.5 \cdot (\mathrm{RMSE}_X + \mathrm{RMSE}_Y) \tag{7}$$

The vertical accuracy is calculated as follows:

$$\textit{Vertical Accuracy} = 1.96 \cdot \mathrm{RMSE}_Z \tag{8}$$

where:

$$\mathrm{RMSE}_Z = \sqrt{\sum \frac{(Z_i - Z_j)^2}{n}} \tag{9}$$

Z_i – the height of observed check point,
Z_j – the height of the orthophoto check point,
n – the number of check points.

3. Results, Validation and Discussion

3.1. Results and Analysis

Figure 8 shows some of the UAV images captured covering different parts of the university campus, while Figures 9 and 10 present the orthophoto of University of Lagos and a portion of the orthophoto at a large scale showing the high-resolution capability of the UAV. The orthophoto was produced at an average ground sampling distance of 4.36 cm. The two figures show a good representation of surface features such as the buildings and car parks. The level of detail captured was more evident in Figure 10 presented at a larger scale given the visibility of cars and other small objects from the photos.

Fig. 8. Images from the UAV:
a) the canal crossing University Road;
b) Chapel of Christ our Light (light-blue roof)
and the Central Mosque (circular dome on top);
c) parked buses (with yellow-coloured tops) at the Shuttle Park;
d) vehicular traffic at the intersection of University Road and Akoka Road

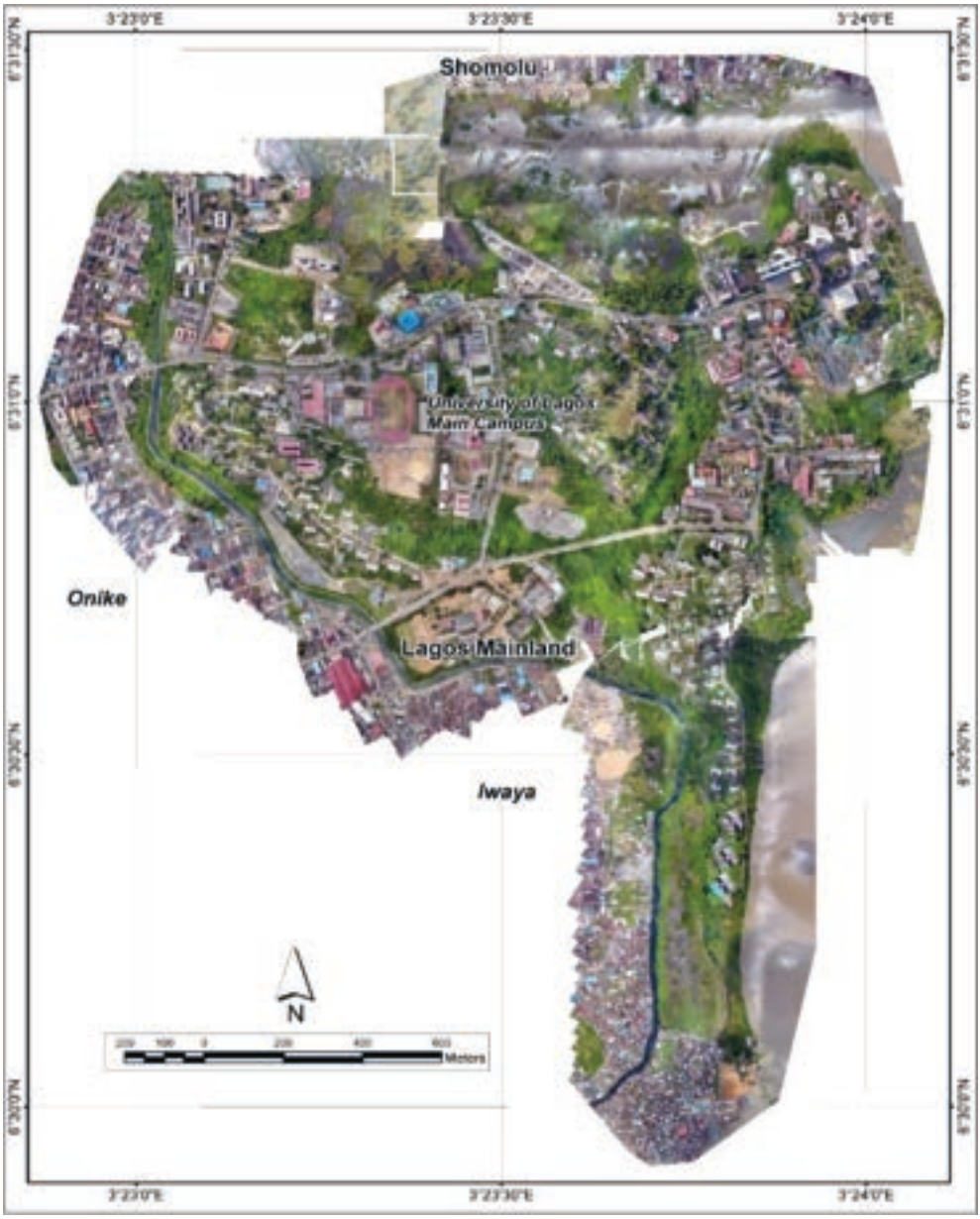

Fig. 9. Orthophoto map of the University of Lagos

Fig. 10. A fragment of the orthophoto shown at a larger scale

Figure 11 presents the DTM for the purpose of height and topography visualisation. The 3D surface model representation of the area is close to reality with the highest point around the Faculty of Science whilst the lowest points are the areas close to the marshy locations and lagoon front such as the rear of Guest House, New Hall and Chapel of Christ our Light. However, slight variations can be observed where there are less dense point clouds, which highlights the importance of a dense point cloud in obtaining a reliable 3D terrain model.

Figure 12 presents the 3D view of University of Lagos where the heights of different structures were shown in diverse colours. The colours depict heights in the range of 0–8.7 m (red), 8.7–12.6 m (orange), 12.6–17.5 m (green), 17.5–24.7 m (leaf green) and ≥24.7 m (blue).

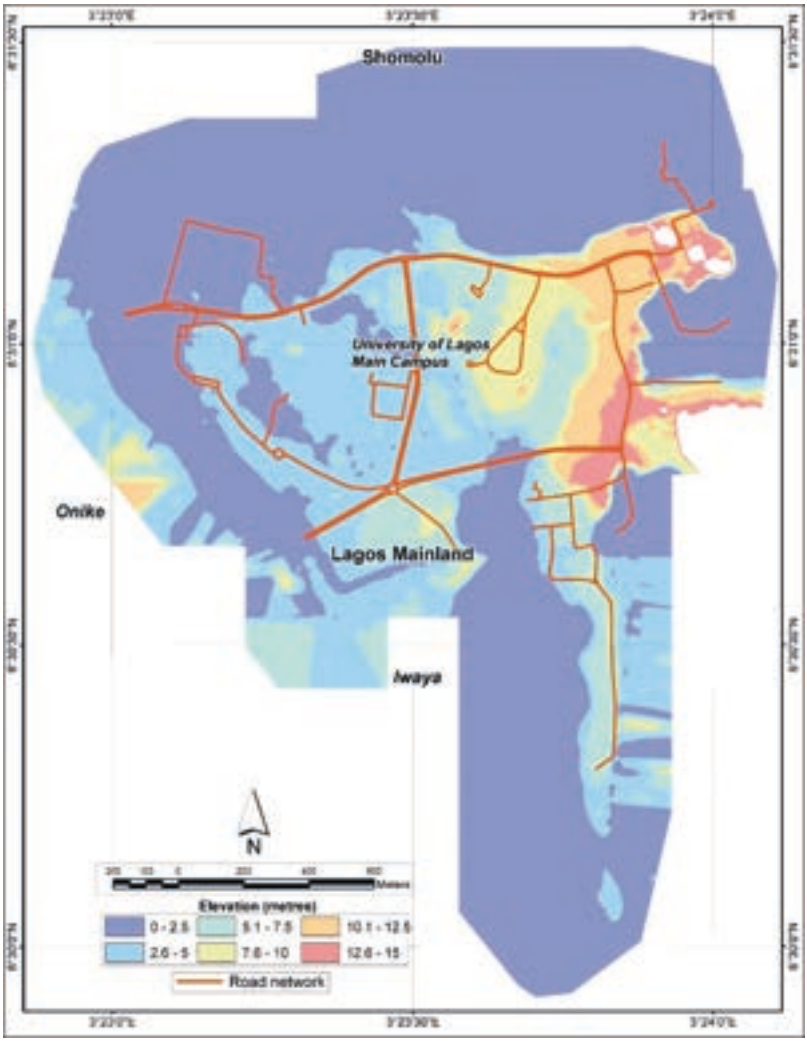

Fig. 11. Digital Terrain Model with an overlay of road network

Some of the structures greater than 24.7 m include the Senate Building and the High-Rise residential quarters. The height variation can aid in decision making such as in this study for the determination of flying height, and planning of surface utility by the University of Lagos Works Department. An attribute query showed that 166 buildings out of 599 (27.71%) are higher than 15 m above mean sea level (m.s.l). This indicates that most of the structures within the university are at a low altitude. Forty-two structures are greater than or equal to 1,000 m^2 in area. This shows that only a small fraction out of the larger population of the university community can be accommodated as residents on campus.

However, the university can maximise the limited land resource by building taller structures rather than smaller ones, to address the current challenges of insufficient staff and student accommodation.

Fig. 12. The 3D View of the buildings with their respective heights

Figure 13 shows the 2019 composite land cover map of the study area, showing the boundary line in grey, road in red, vegetation in green, buildings in pink and water body in blue colour. Analysis shows that the water body occupies 169,336.5 m^2, which covers 7.7% of the total area whilst the vegetation covers 30.2% (665,194 m^2). Seven structures were under construction within the university as at the time of observation.

For a better understanding of the composite map, Table 2 shows the percentage of changes that occurred within the period of study (2015 to 2019). From the table, the statistics showed losses of 15,900 m^2 and 33,167 m^2 in the areas of water body and vegetation respectively. This translates to losses of 3,975.0 m^2/yr and 8,291.8 m^2/yr in the water body and vegetation respectively. If this rate is projected forward, it can be deduced that the loss is significant considering the short duration. The loss is attributed to the gain in buildings and bare land (open ground/grasses) as seen from the table. Within the same 4-year period, there was a 16,306.7 m^2 (4,076.7 m^2/yr) increase in the area of buildings and 32,760.4 m^2 (8,190.1 m^2/yr) increase in open ground/grasses. If the current rate of depletion of vegetation and water bodies is not controlled, this might have a negative impact on the university community in the near future. Accordingly, proper planning and consultation are essential in the allocation of spaces for developmental purposes in order to strike a balance between anthropogenic interventions and ecosystem/biodiversity sustainability.

Fig. 13. 2019 land cover map digitised from the orthophoto

Table 2. Comparison between the base map (2015) and the composite map (2019)

Class	Area – 2015		Area – 2019		Change [m^2]
	[m^2]	[%]	[m^2]	[%]	
Water body	185,236.5	8.4	169,336.5	7.7	−15,900.0
Vegetation	698,361.0	31.7	665,194.0	30.2	−33,167.0
Buildings	212,130.3	9.6	228,436.9	10.4	+16,306.7
Open ground/grasses	1,105,694.8	50.2	1,138,455.2	51.7	+32,760.4
Total	2,201,422.6	100.0	2,201,422.6	100.0	–

3.2. Validation of Results

The validation dataset was based on the static post processed-GNSS derived coordinates of the GCPs. Table 3 shows the point-to-point geolocation details using ten and seven checkpoints indicated in the table as $RMSE_{10}$ and $RMSE_{7}$ respectively. The validation with ten checkpoints showed a lower accuracy, whereas the validation with 7 checkpoints yielded higher accuracy (low RMSEs) in the X, Y and Z coordinates. The values for $RMSE_{10}$ are: 0.978 m, 0.692 m, 2.293 m compared to $RMSE_{7}$ with 0.161 m, 0.206 m, and 0.080 m in the X, Y and Z coordinates respectively. While it is expected that the more the number of control points used, the better the result as observed in [20], in this case the reverse is the case. This is due to the large error contained in three of the control points, particularly in the X and Y coordinates. For example, GME 04 and GME 06 produced errors that are significantly larger than the expected and allowable error of 0.020 m. Therefore, the outlying points were excluded in the final analysis to arrive at a more reasonable result. It is to be noted that the resultant poor quality in the excluded points is attributed to variable factors such as the influence of weather. Accordingly, good climatic conditions devoid of strong wind is considered an important factor that must be taken into consideration in the application of UAV for 3D mapping.

Table 3. Summary of errors in the 3D coordinates

GCP	Accuracy XY/Z [m]	Error X [m]	Error Y [m]	Error Z [m]	Projection error [pixel]
GME04	0.020/0.020	−0.334	0.492	−3.671	0.880
GME06	0.020/0.020	−0.481	0.539	−5.919	0.455
XST347	0.020/0.020	−0.160	0.206	−1.072	0.281
DOS03	0.020/0.020	−3.032	−2.052	1.706	0.627
HRBA	0.020/0.020	0.007	−0.004	0.076	0.512
HRBC	0.020/0.020	−0.007	−0.001	−0.014	0.813
PDUN01	0.020/0.020	−0.002	0.001	0.000	0.763
PDUN03	0.020/0.020	0.003	0.002	0.016	0.202
PDUN05	0.020/0.020	0.001	−0.002	0.002	0.654
PDUN07	0.020/0.020	0.007	0.000	−0.013	0.503
Mean [m]	–	−0.400	−0.082	−0.889	–
Sigma [m]	–	0.892	0.687	2.114	–
$RMSE_{10}$ [m]	–	0.978	0.692	2.293	–
Std. error [m]	–	0.282	0.217	0.668	–
$RMSE_{7}$ [m]	–	0.161	0.206	0.080	–

Summarily, the horizontal and vertical accuracy obtained are 0.183 m and 0.157 m respectively following the application of the second condition, without the assumption of normality and independence in data distribution stated in Section 2.5. Hence, this result suggests a high level of accuracy both in the horizontal and vertical positions on the orthophoto. This accuracy is considerably adequate for 3D mapping and other fit-for-purpose applications such as earth volume determination in engineering works and incidents monitoring and management.

3.3. Discussion of Results

Section 3.2 showed that the data acquired using the UAV technique has a considerable degree of accuracy both in planimetry and height, and as a result is adequate for many fit-for-purpose applications. For example, the acquired images can provide useful information for different applications such as engineering and environmental modelling and monitoring, and emergency assessment. In particular, the orthophotos can be used for mapping, volume computation, displacement analyses, erosion and flood management, disaster management in oil and gas and incident analysis. The DTM generated from the UAV data acquisition can allow quick multi-temporal volume estimations, without the problems of occlusion that can be encountered using terrestrial techniques. The elevation data obtained can be used for cut and fill calculation and development of new structures. For example, the contour plan can be used for engineering design in the university to aid the sand filling of swampy areas (land reclamation), construction of bridges and the design of a good drainage system. Not only that, the backend database will serve as a tool enabling queries to be performed to help in making informed decision on physical developments that include rapid assessment of changes in land use/land cover and new project sites.

4. Conclusions

This study conducted at the University of Lagos has shown that unmanned aerial vehicles (UAVs) have the ability to cover the large gap between terrestrial and aerial methods of mapping and data acquisition. The acquired and processed data from the flight mission can be utilised for different purposes, such as change detection analysis for land use/land cover, terrain modelling and infrastructural planning and monitoring. As would be expected, the result obtained showed that the terrain of University of Lagos is not flat but rather follows a non-uniform undulation as vividly captured from the generated contour map. This contour map is a good asset to the university community in future engineering planning and design. The composite map identified numerous artificial and natural ground features, such as roads, buildings, water bodies, and vegetation. This map is vital in understanding

variations in land use and land development. In the 4-year period between 2015 and 2019, the change detection statistics showed losses of 15,900 m^2 (3,975 m^2/yr) and 33,167 m^2 (8,291.8 m^2/yr) in the areas of water body and vegetation respectively. There was a 16,306.7 m^2 (4,076.7 m^2/yr) increase in the area of buildings and 32,760.4 m^2 (8,190.1 m^2/yr) increase in open ground/grasses within the same period. The losses in water body and vegetation are attributed to the gain in buildings and bare land (open ground/grasses).

Whilst few control points were used for validation, the results obtained showed that UAV 3D mapping is applicable for the acquisition of high-resolution data at a low-cost. Accordingly, it is recommended that this technology can be considered as a fast, safe and cost-effective method of mapping the university landed properties. Also, the topographical and base maps of the institution should be updated at regular intervals for the production of an up-to-date map using this technology. In the process of erecting new structures, the authority concerned should establish as much as possible a balance in the ecosystem, instead of its destruction. The university authorities should also take a bold step in sand-filling part of the inland water-logged area on campus. This would enable the authorities to reclaim such land for future development. Finally, the results from this study should be embraced by the university authorities for future planning and the design of engineering projects within the campus.

Acknowledgements

Special thanks to everyone who contributed to the success of the work and to Pix4D for their free and accessible help files.

References

[1] Nex F., Remondino F.: *UAV for 3D mapping applications: a review.* Applied Geomatics, vol. 6, 2014, pp. 1–15. https://doi.org/10.1007/s12518-013-0120-x.

[2] Zaragoza M.I., Caroti G., Piemonte A., Riedel B., Tengen D., Niemeier W.: *Structure from motion (SfM) processing of UAV images and combination with terrestrial laser scanning, applied for a 3D-documentation in a hazardous situation*. Geomatics, Natural Hazards and Risk, vol. 8, issue 2, 2017, pp. 1492–1504.

[3] Schultz R.J.: *Leveling.* [in:] Brinker R.Ch., Minnick R. (eds.), *The Surveying Handbook*. 2nd ed., Springer Science + Business Media, Dordrech 1995, pp. 113–139.

[4] Wahr J.: *Geodesy and Gravity: Class Notes*. Samizdat Press, Colorado 1996.

[5] Luh H.S.: *High resolution survey for topographic surveying*. IOP Conference Series: Earth and Environmental Science, vol. 18, 2014, 012067. https://doi.org/10.1088/1755-1315/18/1/012067.

[6] Remondino F., Barazzetti L., Nex F., Scaioni M., Sarazzi D.: *UAV Photogrammetry for mapping and 3D modeling – Current status and future perspectives*. International Archives of the Photogrammetry, Remote Sensing and Spatial Information Sciences, vol. XXXVIII-1/C22, 2011, pp. 25–31. https://doi.org/10.5194/isprsarchives-XXXVIII-1-C22-25-2011.

[7] Gustafsson H.: *Unmanned Aerial Vehicles for Geographic Data Capture: A Review.* Examensarbete Teknik, Grundnivå, 15 Hp, Stockholmsverige, 2017. https://www.diva-portal.org/smash/get/diva2:1116742/FULLTEXT01.pdf [access: 27.09.2018].

[8] Lahoti S., Lahoti A., Saito O.: *Application of Unmanned Aerial Vehicle (UAV) for Urban Green Space Mapping in Urbanizing Indian Cities*. [in:] Avtar R., Watanabe T. (eds.), *Unmanned Aerial Vehicle: Applications in Agriculture and Environment*, Springer, Cham 2020, pp. 177–188. https://doi.org/10.1007/978-3-030-27157-2_13.

[9] Iizuka K., Itoh M., Shiodera S., Matsubara T., Dohar M., Watanabe K.: *Advantages of unmanned aerial vehicle (UAV) photogrammetry for landscape analysis compared with satellite data: A case study of postmining sites in Indonesia.* Cogent Geoscience, vol. 4(1), 2018, 1498180. https://doi.org/10.1080/23312041.2018.1498180.

[10] Ruwaimana M., Satyanarayana B., Otero V.M., Muslim A., Syafiq A.M., Ibrahim S. et al.: *The advantages of using drones over space-borne imagery in the mapping of mangrove forests.* PLoS ONE, vol. 13(7), 2018, e0200288. https://doi.org/10.1371/journal.pone.0200288.

[11] Koeva M., Muneza M., Gevaert C., Gerke M., Nex F.: *Using UAVs for map creation and updating. A case study in Rwanda.* Survey Review, vol. 50, issue 361, 2018, pp. 312–325. https://doi.org/10.1080/00396265.2016.1268756.

[12] Sarp G., Erener A., Duzgun S., Sahin K.: *An approach for detection of buildings and changes in buildings using orthophotos and point clouds: A case study of Van Erriş earthquake*. European Journal of Remote Sensing, vol. 47(1), 2014, pp. 627–642.

[13] Qin R.: *An Object-Based Hierarchical Method for Change Detection Using Unmanned Aerial Vehicle Images*. Remote Sensing, vol. 6, 2014, pp. 7911–7932. https://doi.org/10.3390/rs6097911.

[14] Freire S., Santos T., Navarro A., Soares F., Silva J., Afonso N., Fonseca A., Tenedório J.: *Introducing mapping standards in the quality assessment of buildings extracted from very high resolution satellite imagery*. ISPRS Journal of Photogrammetry and Remote Sensing, vol. 90, 2014, pp. 1–9.

[15] Yao H., Qin R., Chen X.: *Unmanned Aerial Vehicle for Remote Sensing Applications – A Review*. Remote Sensing, vol. 11, 2019, 1443. https://doi.org/10.3390/rs11121443.

[16] Akar Ö.: *Mapping land use with using Rotation Forest algorithm from UAV images*. European Journal of Remote Sensing, vol. 50(1), 2017, pp. 269–279. https://doi.org/10.1080/22797254.2017.1319252.

[17] Qian Y.G., Zhou W.Q., Yan J.L., Li W.F., Han L.J.: *Comparing machine learning classifiers for object-based land cover classification using very high resolution imagery*. Remote Sensing, vol. 7(1), 2015, pp. 153–168. https://doi.org/10.3390/rs70100153.

[18] Jumaat N.F.H., Ahmad B., Dutsenwai H.S.: *Land cover change mapping using high resolution satellites and unmanned aerial vehicle*. IOP Conference Series: Earth and Environmental Science, vol. 169(1), 2018, 012076. https://doi.org/10.1088/1755-1315/169/1/012076.

[19] Franklin S.E., Wulder M.A.: *Remote sensing methods in medium spatial resolution satellite data land cover classification of large areas*. Progress in Physical Geography: Earth and Environment, vol. 26(2), 2002, pp. 173–205.

[20] Iheaturu C.J., Ayodele E.G., Okolie C.J.: *An Assessment of the Accuracy of Structure-from-Motion (SfM) Photogrammetry for 3D Terrain Mapping*. Geomatics, Landmanagement and Landscape, no. 2, 2020, pp. 65–82.

[21] Smith M.W., Vericat D.: *From experimental plots to experimental landscapes: topography, erosion and deposition in sub-humid badlands from structure-from-motion photogrammetry*. Earth Surface Processes and Landforms, vol. 40, no. 12, 2015, pp. 1656–1671.

[22] Smith M.W., Carrivick J.L., Quincey D.J.*: Structure from motion photogrammetry in physical geography*. Progress in Physical Geography, vol. 40, no. 2, 2016, pp. 247–275.

[23] NSSDA: *Geospatial Positioning Accuracy Standards. Part 3: National Standard for Spatial Data Accuracy*. Federal Geographic Data Committee Secretariat, Reston, Virginia, 1998. https://www.fgdc.gov/standards/projects/accuracy/part3 [access: 28.10.2020].

[24] Greenwalt C.R., Schultz M.E.: *Principles and Error Theory and Cartographic Applications*. ACIC Technical Report No. 96, Aeronautical Chart and Information Center, U.S. Air Force, St. Louis 1968.